# Peptidomimetic Targeting of Cavbeta2 Overcomes Dysregulation of the L-Type Calcium Channel Density and Recovers Cardiac Function

Francesca Rusconi, Paola Ceriotti, Michele Miragoli, Pierluigi Carullo, Nicolò Salvarani, Marcella Rocchetti, Elisa Di Pasquale, Stefano Rossi, Maddalena Tessari, Silvia Caprari, et al.

# Peptidomimetic Targeting of $Ca_v\beta2$ Overcomes Dysregulation of the L-Type Calcium Channel Density and Recovers Cardiac Function

**BACKGROUND:** L-type calcium channels (LTCCs) play important roles in regulating cardiomyocyte physiology, which is governed by appropriate LTCC trafficking to and density at the cell surface. Factors influencing the expression, half-life, subcellular trafficking, and gating of LTCCs are therefore critically involved in conditions of cardiac physiology and disease.

**METHODS:** Yeast 2-hybrid screenings, biochemical and molecular evaluations, protein interaction assays, fluorescence microscopy, structural molecular modeling, and functional studies were used to investigate the molecular mechanisms through which the LTCC $Ca_v\beta2$ chaperone regulates channel density at the plasma membrane.

**RESULTS:** On the basis of our previous results, we found a direct linear correlation between the total amount of the LTCC pore-forming $Ca_v\alpha1.2$ and the Akt-dependent phosphorylation status of $Ca_v\beta2$ both in a mouse model of diabetic cardiac disease and in 6 diabetic and 7 nondiabetic cardiomyopathy patients with aortic stenosis undergoing aortic valve replacement. Mechanistically, we demonstrate that a conformational change in $Ca_v\beta2$ triggered by Akt phosphorylation increases LTCC density at the cardiac plasma membrane, and thus the inward calcium current, through a complex pathway involving reduction of $Ca_v\alpha1.2$ retrograde trafficking and protein degradation through the prevention of dynamin-mediated LTCC endocytosis; promotion of $Ca_v\alpha1.2$ anterograde trafficking by blocking Kir/Gem-dependent sequestration of $Ca_v\beta2$, thus facilitating the chaperoning of $Ca_v\alpha1.2$; and promotion of $Ca_v\alpha1.2$ transcription by the prevention of Kir/Gem-mediated shuttling of $Ca_v\beta2$ to the nucleus, where it limits the transcription of $Ca_v\alpha1.2$ through recruitment of the heterochromatin protein $1\gamma$ epigenetic repressor to the *Cacna1c* promoter. On the basis of this mechanism, we developed a novel mimetic peptide that, through targeting of $Ca_v\beta2$, corrects LTCC life-cycle alterations, facilitating the proper function of cardiac cells. Delivery of mimetic peptide into a mouse model of diabetic cardiac disease associated with LTCC abnormalities restored impaired calcium balance and recovered cardiac function.

**CONCLUSIONS:** We have uncovered novel mechanisms modulating LTCC trafficking and life cycle and provide proof of concept for the use of $Ca_v\beta2$ mimetic peptide as a novel therapeutic tool for the improvement of cardiac conditions correlated with alterations in LTCC levels and function.

Francesca Rusconi, PhD*
Paola Ceriotti, BsC*
Michele Miragoli, PhD
Pierluigi Carullo, BsC
Nicolò Salvarani, PhD
Marcella Rocchetti, PhD
Elisa Di Pasquale, PhD
Stefano Rossi, PhD
Maddalena Tessari, MSc, PhD
Silvia Caprari, PhD
Magali Cazade, PhD
Paolo Kunderfranco, PhD
Jean Chemin, PhD
Marie-Louise Bang, PhD
Fabio Polticelli, PhD
Antonio Zaza, PhD
Giuseppe Faggian, MD
Gianluigi Condorelli, MD, PhD
Daniele Catalucci, PhD

*Dr Rusconi and P. Ceriotti contributed equally to this work.

**Correspondence to:** Daniele Catalucci, PhD, National Research Council, Institute of Genetic and Biomedical Research, and Humanitas Clinical and Research Center, Via Manzoni , 113, 20089 Rozzano, Milan, Italy. E-mail daniele.catalucci@cnr.it

Sources of Funding, see page 544

**Key Words:** calcium ■ calcium channels, L-type ■ cardiovascular diseases ■ diabetic cardiomyopathies ■ drug therapy ■ peptides ■ protein transport

## Clinical Perspective

### What Is New?

- A tight control of the $Ca^{2+}$ cardiac machinery is essential for normal cardiac physiology. Alterations in the voltage-dependent L-type calcium channel (LTCC), the key mediator of intracellular $Ca^{2+}$ entry, are associated with various life-threatening cardiovascular conditions such as pathologic hypertrophy, atrial fibrillation, post-inflammatory cardiomiopathy, hypertension, and diabetic cardiomyopathy. The potential use of positive $Ca^{2+}$ modulators for the treatment of cardiovascular pathologies has received considerable attention during the past decades. However, hitherto, pharmacologic approaches aimed at enhancing $Ca^{2+}$ current and inotropism in systolic heart failure have frequently been found to favor arrhythmogenesis and diastolic dysfunction, thereby limiting their use in the clinic.
- Here, we identified a novel peptidomimetic therapeutic tool for the treatment of cardiovascular diseases that, via an unconventional mechanism, bypasses the arrhythmogenic limitations of current channel-activator inotropes. In particular, by dissecting new regulatory pathways modulating the LTCC life cycle, we generated a mimetic peptide that, through multiple levels of regulation, specifically targets the LTCC $Ca_v\beta2$ cytosolic chaperone, thereby controlling LTCC assembly and density at the plasma membrane while preserving its physiologic channel function.

### What Are the Clinical Implications?

- We provide proof of concept for the exploitation of a novel therapy based on mimetic peptide technology and demonstrate that cardiac dysfunctions (eg, diabetic cardiomyopathy) associated with LTCC abnormalities can be effectively treated by in vivo administration of the generated mimetic peptide. Thus, mimetic peptide technology associated with nanocarriers for safe and cardiac-specific delivery may provide novel innovative therapeutic tools for the treatment of cardiac diseases.

Maintenance of calcium homeostasis is critical for preserving the physiology of the cell. A variety of complex mechanisms intervene in the regulation of intracellular levels of $Ca^{2+}$ and its compartmentalization between subcellular compartments. In the heart, $Ca^{2+}$ release from the sarcoplasmic reticulum (SR), the major intracellular $Ca^{2+}$ store, to the cytosol is regulated through a process called $Ca^{2+}$-induced $Ca^{2+}$ release.[1,2] $Ca^{2+}$-induced $Ca^{2+}$ release is initiated by the entry of $Ca^{2+}$ into cardiac cells through sarcolemmal voltage-dependent L-type $Ca^{2+}$ channels (LTCCs), which triggers the release of $Ca^{2+}$ from the SR to the cytoplasm through ryanodine receptor 2. A close association between LTCC and ryanodine receptor 2 is required for efficient $Ca^{2+}$-induced $Ca^{2+}$ release and is dependent on the density and organization of LTCCs within the T-tubular invagination of the plasma membrane.[2] The increase in free intracellular $Ca^{2+}$ allows $Ca^{2+}$ to bind to troponin C, initiating muscle contraction. This is terminated subsequently by the removal of cytosolic $Ca^{2+}$ through its reuptake into the SR via the cardiac SR $Ca^{2+}$-ATPase and, to a lesser extent, by other $Ca^{2+}$ transport systems. This process is a key regulator of cardiac excitation-contraction coupling and a major determinant for intrinsic physiologic properties of the beating heart.

Modifications in the appropriate trafficking of LTCC to and density at the cell surface and changes in its subcellular localization and gating properties can cause functional alterations in the overall inward $Ca^{2+}$ current ($I_{Ca,L}$)[3] and consequently the cellular $Ca^{2+}$ machinery. In line with this, acquired and genetically determined LTCC dysfunction has been found to be associated with various human diseases,[4] including life-threatening cardiovascular pathologies.[4–14]

LTCCs are expressed in all excitable cells (ie, striated, smooth muscle, and neuronal cells).[15] The cardiac LTCC is composed of the pore-forming $Ca_v\alpha1.2$ and the accessory $Ca_v\beta2$ and $Ca_v\alpha2\delta$ subunits.[15–17] $Ca_v\beta2$, the cytoplasmic chaperone of $Ca_v\alpha1.2$, is composed of a globular domain (including an Src homology 3 [SH3] and a guanylate kinase-like [GK] domain) and a C-terminal coiled-coil tail (C-tail) and belongs to the membrane-associated GK family, which is involved in intracellular signaling and the establishment/maintenance of cell polarity.[16] $Ca_v\beta2$ binds to the pore unit at the $\alpha$-interaction domain,[18] affecting its trafficking to the plasma-membrane,[19–21] its internalization,[22] and its gating properties.[17,23] However, although LTCC channel physiology has been intensively studied during the last decades, more in-depth insights into the mechanisms regulating the trafficking and function of LTCCs are still required. Here, we unraveled new regulatory pathways modulating the LTCC life cycle and generated a mimetic peptide (MP) that, through multiple levels of regulation, specifically targets $Ca_v\beta2$, thereby controlling LTCC levels at the plasma membrane. Additionally, we provide proof of concept for in vivo administration of MP as an effective therapeutic strategy for the treatment of cardiac disorders associated with LTCC abnormalities.

## METHODS

Detailed procedures are provided in the online-only Data Supplement.

### Plasmids

Yeast 2-hybrid bait constructs were generated in the pGBKT7 vector (Clontech), and the mouse adult heart cDNA library was generated with the Make Your Own Mate & Plate Library System (Clontech). For the nanoluciferase and bioluminescence

resonance energy transfer (BRET) assays, cDNAs were cloned into the pNLF1-N and pNLF1-N and the HaloTag- pFN21A vector (Promega), respectively.

## Western and Dot Blot Analyses

$Ca_v\alpha1.2$ $Ca_v\beta2$ (S8b-1), HA, and transferrin receptor were from Abcam; c-myc 9E10 was from Santa Cruz; HP-1$\gamma$ 42S2 came from Millipore; GAPDH 14C10 was purchased from Cell Signaling Technology; Polyaginine 9R was from Cell Applications; and goat anti-mouse and anti-rabbit horseradish peroxidase was purchased from Thermo Fisher Scientific. A rabbit polyclonal antibody against the phosphorylated Akt consensus site of $Ca_v\beta2$ was generated by GenScript.

## Nanoluciferase Assay

In NanoLuc Luciferase (Promega), HEK293 cells pretreated for 30 minutes with 20 μmol/L cycloheximide were transfected as described in the Results section. Time-course analysis was performed with a Synergy 4 instrument (BioTek).

## NanoBRET Assay

In the NanoBRET Assay (Promega), HEK293-transfected cells were treated with 100 nmol/L NanoBRET 618 ligand, and signals were detected 5 hours after treatment. For the peptide-protein binding assay, tetramethylrhodamine peptides were used. Signals were detected with a Synergy 4 instrument (BioTek).

## Human Patients

Patients with aortic stenosis who underwent aortic valve replacement were recruited retrospectively from the biobank available at the University Hospital of Verona, Division of Cardiac Surgery, Verona, Italy. Approval for studies on human tissue samples was obtained from the ethics committee of the University Hospital of Verona. All patients or their relatives gave informed consent before surgery.

## Animals

All procedures on mice were performed according to institutional guidelines in compliance with national (D.L. N.26, 04/03/2014) and international law and policies (new directive 2010/63/EU). The protocol was approved by the Italian Ministry of Health. Special attention was paid to animal welfare to minimize the number of animals used and their suffering. All experiments were performed on 12-week-old male mice with at least 8 animals per group. Diabetes mellitus was induced in adult C57B6/J male mice by intraperitoneal injection of streptozotocin (50 $mg \cdot kg^{-1} \cdot d^{-1}$) for 5 days. At 2 weeks after the last injection of streptozotocin, whole blood was obtained and glucose levels were measured with the Accu-Chek active blood glucose monitoring system (Roche). Mice with hyperglycemia (>300 mg/dL) were used for the study. Citrate buffer–treated mice were used as nondiabetic controls. After streptozotocin treatment, mice were treated with peptides (2.5 $mg \cdot kg^{-1} \cdot d^{-1}$ IP) as described in the Results section.

## Statistical Analysis

Data are presented as mean±SD. The normality of the data was assessed with the Kolmogorov-Smirnov test. Statistical comparison was performed in at least 3 independent experiments with the Mann-Whitney test, and comparisons between groups were analyzed by repeated-measures ANOVA combined with the Tukey multicomparison. The Pearson correlation coefficient test was used for the analysis of human data. Prism 6.0 software (GraphPad Software) was used to assess the normality of the data and for statistical calculation. A value of $P<0.05$ was considered significant.

# RESULTS

## $Ca_v\beta2$ Molecular Reorganization Stabilizes $Ca_v\alpha1$

We previously demonstrated that $Ca_v\alpha1.2$ total protein levels are affected by the phosphorylation status of $Ca_v\beta2$ at the Akt consensus site in its C-tail.[24] To determine the mechanism by which phosphorylated $Ca_v\beta2$ controls the $Ca_v\alpha1.2$ level, we performed yeast 2-hybrid screenings of human and mouse heart cDNA libraries using phosphomimetic $Ca_v\beta2$ ($Ca_v\beta2$-SE[24]) as bait. Unexpectedly, several positive clones corresponded to the SH3 region in the globular domain of $Ca_v\beta2$ (Figure 1A), and cotransformation assays confirmed the binding of $Ca_v\beta2$-SE, but not wild-type $Ca_v\beta2$, to the globular region of $Ca_v\beta2$ (Figure 1B). The specificity of the interaction was further confirmed by coimmunoprecipitation assays (Figure 1C). Analysis of the $Ca_v\beta2$ structure revealed a solvent accessible sequence within the minimal common region of the identified $Ca_v\beta2$ clones (Figure 1A), which we predicted to be responsible for the binding to the $Ca_v\beta2$ C-tail on Akt phosphorylation. Taken together, these results suggest that the Akt-dependent protective effect on $Ca_v\alpha1.2$ stability is not mediated through interaction with other proteins but relies entirely on $Ca_v\beta2$ structural rearrangements, triggered by Akt-mediated phosphorylation of its C- allowing interaction with a minimal region within the $Ca_v\beta2$-SH3 globular domain that we called the tail-interacting domain (TID).

To determine whether the TID directly affects $Ca_v\alpha1.2$ protein stability, we used site-specific mutagenesis to replace positively charged lysines (K) at positions 141, 149, and 161 in the TID sequence with glutamines (Q) to destroy any potential ionic interaction between the TID and the C-tail. In cells cotransfected with $Ca_v\alpha1.2$ and $Ca_v\beta2$-SE, similar protein levels of $Ca_v\alpha1.2$ were found in the presence and absence of Akt activation (ie, with and without serum, corresponding to phosphorylated and nonphosphorylated $Ca_v\beta2$, respectively; Figure 1F, inset), whereas significantly reduced $Ca_v\alpha1.2$ levels were found in cells cotransfected with K161Q-mutant $Ca_v\beta2$-SE under serum free conditions (Figure 1D). Consistently, the K161Q mutation prevented the interaction with $Ca_v\beta2$-SE in the yeast 2-hybrid

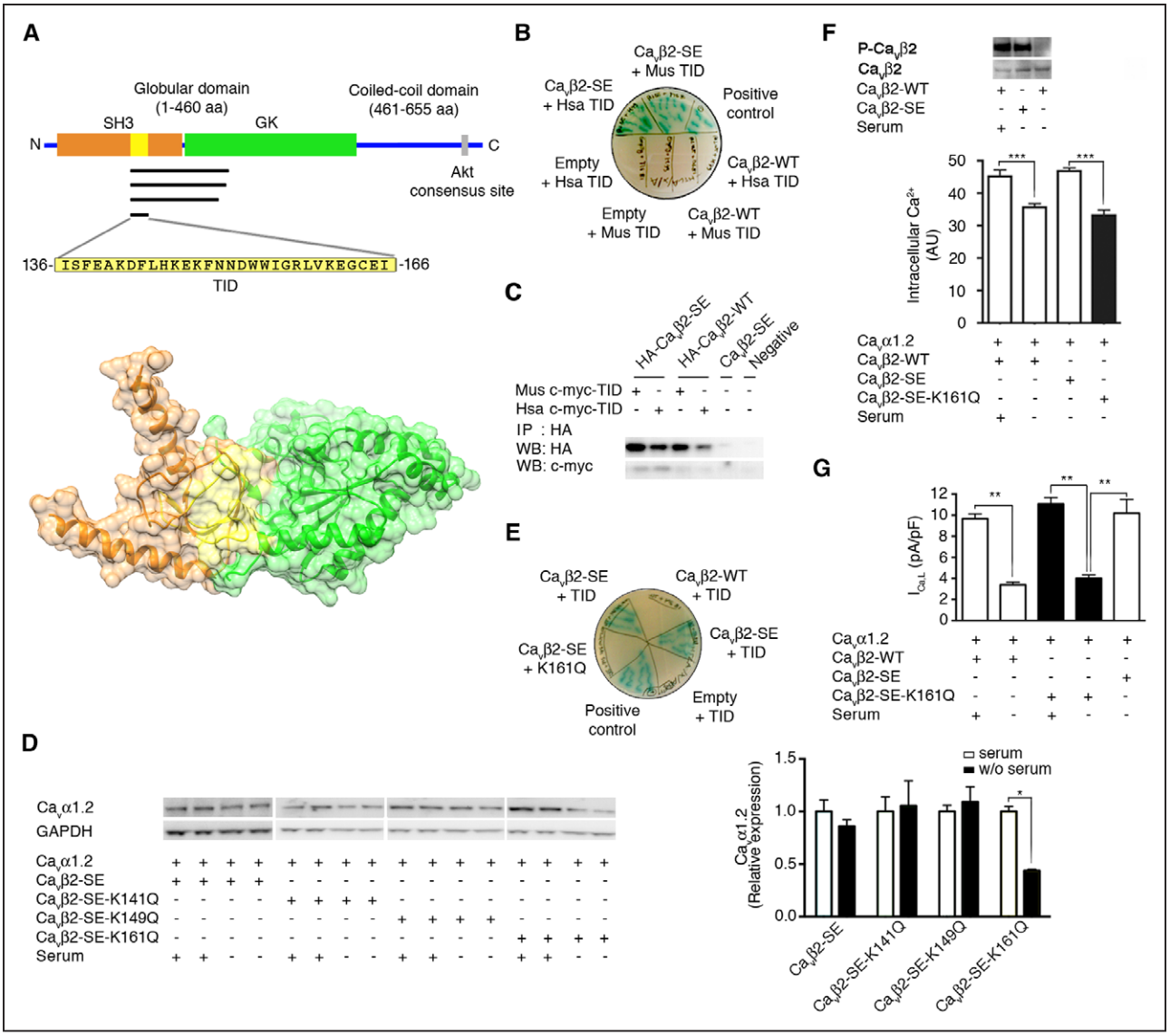


**Figure 1. Identification of a new binding region in the Src homology 3 (SH3) domain of $Ca_V\beta2$.**
**A**, **Top**, Schematic representation of the $Ca_V\beta2$ domain structure (brown and green boxes, SH3 and guanylate kinase-like [GK] globular domains, respectively; blue line, coiled-coil region; yellow box, tail-interacting domain [TID]; gray bar, Akt consensus site). Black lines represent the clones identified by the yeast 2-hybrid screening. **Bottom**, Three-dimensional structure showing the protein backbone (brown, SH3; green, GK) and accessible surface of the TID (yellow). **B**, Yeast 2-hybrid cotransformation assay. Labels refer to bait and prey plasmids transformed into yeast cells. Hsa indicates human; and Mus, mouse. **C**, Coimmunoprecipitation (IP) assay in HEK293 cells. Representative experiments are shown (n=6). **D**, Western blot (WB) analysis (**left**) and densitometry (**right**) for $Ca_V\alpha1.2$ in total protein lysates from HEK293 cells transfected as indicated (n=4; Mann-Whitney test). **E**, Yeast 2-hybrid cotransformation assay. Labels refer to bait and prey plasmids transformed into yeast cells. **F**, **Top,** Western blot analysis for the phosphorylation status of $Ca_V\beta2$ at the Akt consensus site in total protein lysates from HEK293 cells transfected as indicated (n=3). **Bottom,** Intracellular $Ca^{2+}$ levels in serum starved HEK293 cells transfected as indicated (n=8; 1-way ANOVA). AU indicates arbitrary units. **G**, $Ca^{2+}$ current measurements in serum-starved tSA201 cells transfected as indicated (n=15). All data are shown as mean±SD. $*P<0.05$; $**P<0.01$; $***P<0.001$.

system (Figure 1E), suggesting a direct role of the TID in the protective effect of $Ca_V\beta2$-SE on $Ca_V\alpha1.2$ stability. Similarly, the intracellular $Ca^{2+}$ concentration was significantly higher in cells cotransfected with $Ca_V\alpha1.2$ and $Ca_V\beta2$-SE compared with wild-type $Ca_V\beta2$ after serum starvation, whereas cotransfection with K161Q-mutant $Ca_V\beta2$-SE ablated this effect (Figure 1F). In addition, $I_{Ca,L}$ was significantly reduced in cells transfected with K161Q-mutant $Ca_V\beta2$-SE compared with $Ca_V\beta2$-SE (Figure 1G). Taken together, these results provide evidence that the TID within the $Ca_V\beta2$-SH3 domain plays a direct role in stabilizing $Ca_V\alpha1.2$.

## MP Affects LTCC Protein Stability and Function In Vitro

We next designed an array of partially overlapping peptides covering the C-tail and tested their effect on $Ca_v\alpha1.2$ stability through binding to the $Ca_v\beta2$-TID. Cotransfection of cells with $Ca_v\alpha1.2$, $Ca_v\beta2$, and individual peptides, followed by Western blot analyses (Figure 2A) and intracellular $Ca^{2+}$ concentration measurements (Figure 2B), identified several peptides that efficiently regulated $Ca_v\alpha1.2$ protein amounts and increased intracellular $Ca^{2+}$ concentration without inducing apoptosis (Figure 2A). For our subsequent studies, we selected peptide 11 designated as MP, the effect of which was most similar to that of $Ca_v\beta2$-SE. Computational docking simulation of the interaction between the MP and the $Ca_v\beta2$-TID (Figure 2C) and additional site-specific mutagenesis (Figure I in the online-only Data Supplement) further defined the TID-MP binding pocket.

Next, to facilitate intracellular uptake, MP was fused to an oligoarginine (R7W) cell-penetrating peptide.[25] The R7W was fused to the N-terminus of the MP, which, on the basis of the $Ca_v\beta2$-MP 3D model (Figure 2C), was not predicted to create steric hindrance or to affect MP function. To monitor the extent and specificity by which R7W-MP binds to $Ca_v\beta2$, we performed a BRET protein interaction assay between a $Ca_v\beta2$-NanoLuc donor and increasing doses of R7W-MP or R7W-scramble peptide conjugated to the tetramethylrhodamine fluorophore (acceptor). This revealed binding of R7W-MP to $Ca_v\beta2$ in a dose-dependent manner, a finding specific for the $Ca_v\beta2$-SH3 domain and not the GK domain (Figure 2D). Dot blot analyses after $Ca_v\beta2$ immunoprecipitation on lysates from cells transfected with $Ca_v\beta2$ constructs and treated with R7W-peptides supported the above results (Figure IIA in the online-only Data Supplement). Furthermore,

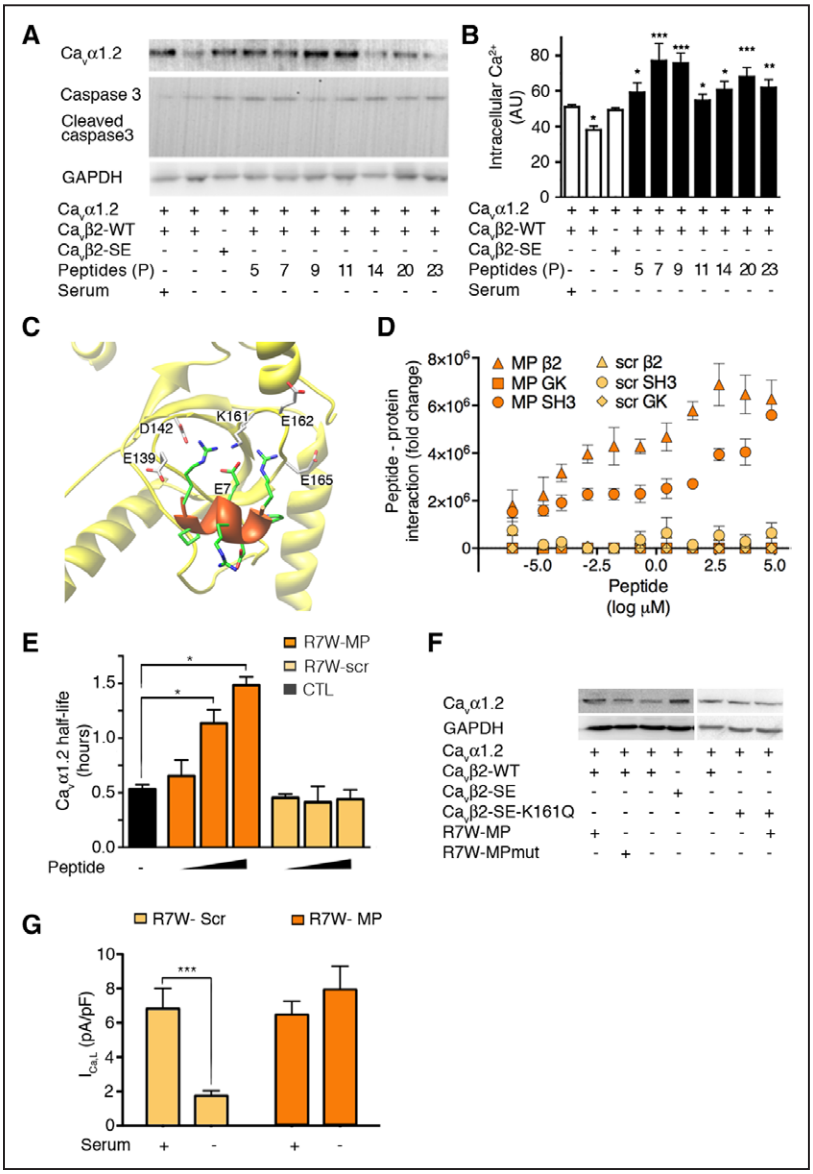


**Figure 2. The mimetic peptide (MP) R7W-MP binds to $Ca_v\beta2$ and affects $Ca_v\alpha1.2$ protein stability and function.** **A**, Western blot analysis of $Ca_v\alpha1.2$ and Caspase 3 in total protein lysates from HEK293 cells transfected as indicated (n=3). **B**, Intracellular $Ca^{2+}$ levels in HEK293 cells transfected as indicated (n=8; 1-way ANOVA). **C**, Molecular model of the MP (orange) docked onto the tail-interacting domain (TID) region of $Ca_v\beta2$ (yellow), revealing the formation of electrostatic interactions. **D**, Dose-dependent binding of R7W-MP-tetramethylrhodamine (TMR) and R7W-scramble (R7W-scr)–TMR to $Ca_v\beta2$-NanoLuc, Src homology 3 (SH3)–NanoLuc, and guanylate kinase-like (GK)–NanoLuc as measured by bioluminescence resonance energy transfer assay in transfected HEK293 cells (n=6). **E**, $Ca_v\alpha1.2$ half-life measured by a NanoLuc luciferase assay. HEK293 cells were transfected with $Ca_v\alpha1.2$-NanoLuc and treated with incremental doses (0.12, 1.3, and 10,2 μmol/L) of R7W-MP and R7W-scr as indicated (n=6; 1-way ANOVA). **F**, Western blot analysis for $Ca_v\alpha1.2$ in total protein lysates from serum-starved HEK293 cells transfected and treated as indicated (n=4; Mann-Whitney test). **G**, $Ca^{2+}$ current measurements in tSA201 cells transfected and treated as indicated (n=15; 1-way ANOVA). All data are shown as mean±SD. **P*<0.05; ***P*<0.01; ****P*<0.001.

R7W-MP was found to colocalize with $Ca_v\beta2$ in adult cardiomyocytes (Figure IIB in the online-only Data Supplement). As expected, R7W-MP was shown to increase the half-life (Figure 2E) and total protein levels (Figure IIC in the online-only Data Supplement) of $Ca_v\alpha1.2$ in a dose-dependent manner. Replacement of either K161 in the TID sequence or its direct interacting residue in MP (E7) with glutamines (Q) ablated the protective effect of R7W-MP on $Ca_v\alpha1.2$ protein levels (Figure 2F) and half-life (Figure IID in the online-only Data Supplement), confirming the specificity of the TID-MP interaction. R7W-MP, but not R7W-scramble, was found to efficiently preserve $I_{Ca,L}$ (Figure 2G) without affecting the steady-state voltage dependency of the channel under serum free conditions (data not shown).

## R7W-MP Prevents Dynamin From Binding to $Ca_v\beta2$ and Protects $Ca_v\alpha1.2$ From Protein Degradation

The $Ca_v\beta2$-SH3 domain was previously shown to downregulate LTCC density at the plasma membrane through interaction with dynamin, a GTPase involved in endocytosis and vesiculation.[22] Furthermore, a dynamin-specific inhibitor was found to protect $Ca_v\alpha1.2$ from protein degradation[22] and to extend its half-life (data not shown). This led us to question whether R7W-MP might compete with dynamin for binding to the $Ca_v\beta2$-SH3 domain, thereby enhancing the $Ca_v\alpha1.2$ half-life. To test this hypothesis, we performed a BRET assay that revealed that R7W-MP indeed prevents dynamin from binding to $Ca_v\beta2$ (Figure 3A). In addition, we demonstrated that $Ca_v\beta2$ dissociates from $Ca_v\alpha1.2$ when bound to dynamin, whereas R7W-MP recovered the interaction of $Ca_v\alpha1.2$ with its chaperone (Figure 3B). Finally, in a cell surface protein biotinylation assay, a significant reduction in biotinylated $Ca_v\alpha1.2$ (membrane fraction) was found in cells cotransfected with dynamin, an effect that was fully counteracted by R7W-MP (Figure 3C).

## R7W-MP Facilitates $Ca_v\alpha1.2$ Chaperoning to the Plasma Membrane by Preventing Kir/Gem Binding to $Ca_v\beta2$

Kir/Gem, together with Rad, Rem, and Rem2, is a member of the RGK small GTP-binding protein family[26] known to negatively affect the amount of LTCCs at the cell surface.[27,28] In particular, overexpression of Kir/Gem in *Xenopus* oocytes was reported to compromise the association of $Ca_v\beta3$ with $Ca_v\alpha1.2$ and to prevent the trafficking of the channel to the plasma membrane by sequestering $Ca_v\beta3$ in intracellular compartments.[27] From this finding and evidence that Kir/Gem binds to $Ca_v\beta3$ through a region within its SH3 domain,[29] we hypothesized that R7W-MP promotes anterograde trafficking of $Ca_v\alpha1.2$ by preventing Kir/Gem from complexing with $Ca_v\beta2$. A BRET interaction assay confirmed the binding of Kir/Gem to $Ca_v\beta2$, which was compromised by R7W-MP (Figure 4A). In addition, the association of $Ca_v\beta2$ with $Ca_v\alpha1.2$, which was drastically affected by the presence of Kir/Gem, was gradually recovered by R7W-MP (Figure 4B). The above results were supported by a surface protein biotinylation assay showing that R7W-MP treatment is sufficient to prevent the Kir/Gem-mediated reduction of $Ca_v\alpha1.2$ at the plasma membrane (Figure 4C).

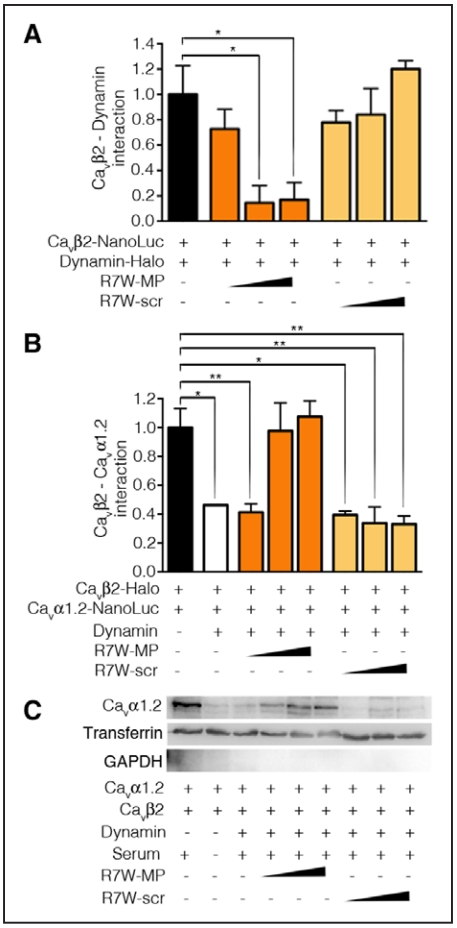


**Figure 3. R7W–mimetic peptide (MP) prevents dynamin from binding to $Ca_v\beta2$ and enhances $Ca_v\alpha1.2$ density at the plasma membrane.**
**A**, $Ca_v\beta2$-dynamin protein affinity as measured by bioluminescence resonance energy transfer (BRET) assay in HEK293 cells transfected with $Ca_v\beta2$-NanoLuc and Dynamin-Halo and treated as indicated (n=6). **B**, $Ca_v\beta2$-$Ca_v\alpha1.2$ protein affinity as measured by BRET assay in HEK293 cells transfected with $Ca_v\beta2$-Halo and $Ca_v\alpha1.2$-NanoLuc and treated as indicated (n=6). **C**, Cell surface biotinylation assay performed in HEK293 cells transfected and treated as indicated (n=4). All data are shown as mean±SD. Peptide doses were 0.12, 1.3, and 10.2 μmol/L. R7W-scr indicates R7W-scramble. **P*<0.05; ***P*<0.01 (Mann-Whitney test).

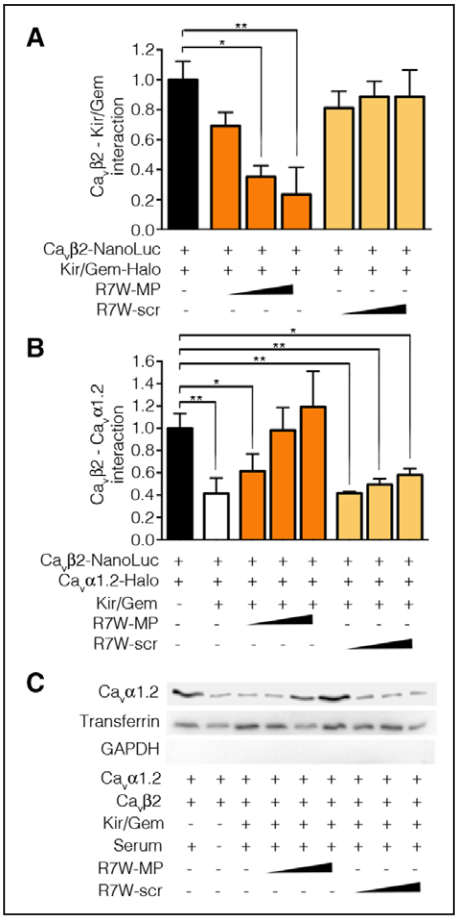


**Figure 4. R7W–mimetic peptide (MP) prevents Kir/Gem from binding to $Ca_v\beta2$ and enhances $Ca_v\alpha1.2$ density at the plasma membrane.**

**A**, $Ca_v\beta2$-Kir/Gem protein affinity as measured by bioluminescence resonance energy transfer (BRET) assay in HEK293 cells treated as indicated (n=6). **B**, $Ca_v\beta2$-$Ca_v\alpha1.2$ protein affinity as measured by BRET assay in HEK293 cells treated as indicated (n=6). **C**, Cell surface biotinylation assay performed in HEK293 cells transfected and treated as indicated (n=6). All data are shown as mean±SD. Peptide doses were 0.12, 1.3, and 10.2 μmol/L. R7W-scr indicates R7W-scramble. **P*<0.05; ***P*<0.01 (Mann-Whitney test).

## R7W-MP Prevents Kir/Gem-Mediated Relocation of $Ca_v\beta2$ to the Nucleus and Promotes *cacna1* Expression

Members of the RGK family show several nuclear import signals and have been reported to sequester and shuttle $Ca_v\beta3$ and $Ca_v\beta4$ from the cytoplasm to the nucleus.[30,31] In addition, $Ca_v\beta1b$, $Ca_v\beta4$, and $Ca_v\beta3$ were shown to interact with nuclear proteins and to modulate gene expression. In particular, the $Ca_v\beta4$ short splice variant in brain was found to interact with the nuclear heterochromatin protein 1γ (HP1γ),[30] a member of the chromatin organization modifier superfamily, negatively regulating gene expression.[32] Thus, we hypothesized that, when bound to Kir/Gem, cytoplasmic $Ca_v\beta2$ relocates to the nucleus, where it affects the transcription of a specific set of genes through recruitment of HP1γ. As predicted, overexpression of Kir/Gem in HL-1 cardiac cells resulted in the translocation of $Ca_v\beta2$ from the cytosol/plasma membrane to the nucleus, where it was found to colocalize with HP1γ (Figure 5A). The specific interaction between $Ca_v\beta2$ and HP1γ was confirmed by BRET (Figure 5B) and coimmunoprecipitation (Figure 5C) assays, whereas R7W-MP prevented the interaction (Figure 5B and 5C). In contrast, $Ca_v\beta2$ did not interact with bromodomain 4,[33] an epigenetic factor that facilitates transcriptional activation (Figure III in the online-only Data Supplement). Taken together, these data point to a specific interaction between the nucleus-relocalized $Ca_v\beta2$ and HP1γ that is potentially required for the regulation of specific genes.

In muscle progenitor cells, $Ca_v\beta1$ was recently shown to translocate to the nucleus and to regulate gene expression by recognizing noncanonical heptameric sites at the promoter region of a number of genes.[34] To determine whether nuclear $Ca_v\beta2$ might play a similar role and be part of a negative feedback loop in cardiac cells by regulating genes encoding LTCC subunits, we performed promoter analysis that identified 3 and 1 noncanonical sequences in the promoter region of *Cacna1c* (encoding $Ca_v\alpha1.2$) and *Cacnb2* (encoding $Ca_v\beta2$), respectively (Figure 5F and data not shown). Consistently, $Ca_v\alpha1.2$ RNA levels were found to be reduced in Kir/Gem-transfected HL-1 cells (causing translocation of $Ca_v\beta2$ to the nucleus), whereas $Ca_v\alpha1.2$ expression was recovered by R7W-MP treatment (Figure 5D). In contrast, $Ca_v\beta2$ expression was unaltered under all analyzed conditions (data not shown). Cotransfection with HP1γ-specific RNAi (Figure IV in the online-only Data Supplement) prevented the reduction in $Ca_v\alpha1.2$ RNA levels (Figure 5E), demonstrating that the ability of nuclear $Ca_v\beta2$ to repress LTCC pore unit expression is dependent on its interaction with HP1γ. Consistent with a direct role of nuclear $Ca_v\beta2$ in regulating *Cacna1c* gene expression, chromatin immunoprecipitation with $Ca_v\beta2$ antibody, followed by quantitative polymerase chain reaction analysis for the above promoter sequences revealed enrichment for the NC1 site at the *Cacna1c* promoter, which was prevented by R7W-MP treatment (Figure 5F). Furthermore, a luciferase-based promoter assay confirmed the negative regulatory effect of nuclear $Ca_v\beta2$ on *Cacna1* gene expression (Figure 5G), supporting the idea that relocalized $Ca_v\beta2$ contributes to adjusting channel density in cells via a negative feedback loop.

## R7W-MP Restores Cardiac Function In Vivo Through Modulation of LTCC

Our next objective was to explore the use of R7W-MP for potential cardiac treatments in vivo. After dot blot

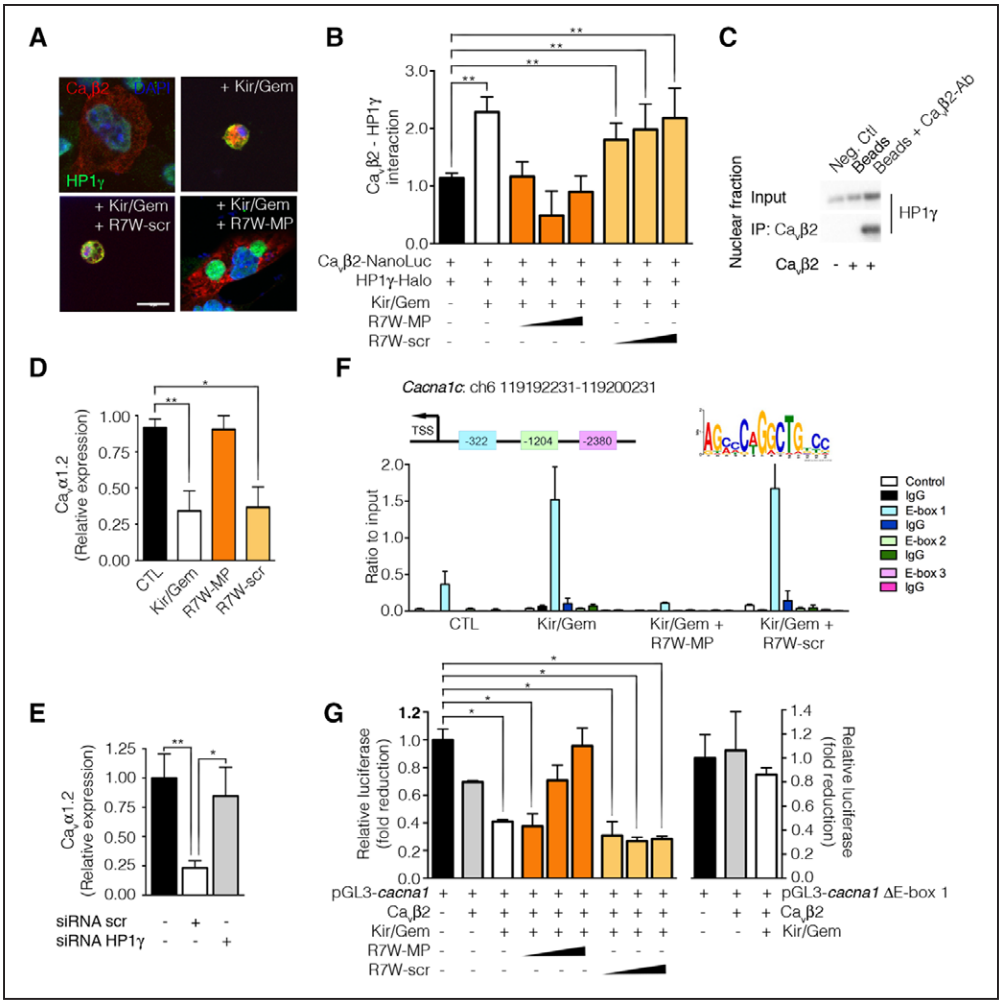


**Figure 5. R7W–mimetic peptide (MP) prevents relocation of $Ca_v\beta2$ to the nucleus and promotes *cacna1* expression.** **A**, Immunofluorescence of $Ca_v\beta2$ (red) and heterochromatin protein 1γ (HP1γ; green) in HL-1 cells transiently transfected with $Ca_v\beta2$-DsRed and Kir/Gem constructs and treated as indicated. Bar=10 μm (n=15). **B**, $Ca_v\beta2$-Hp1γ protein interaction as measured by bioluminescence resonance energy transfer (BRET) assay in HEK293 cells transfected with $Ca_v\beta2$-NanoLuc and Hp1γ-Halo and treated as indicated (n=6). **C**, Coimmunoprecipitation assay from the nuclear fraction of HEK293 cells, confirming the interaction of Hp1γ with $Ca_v\beta2$. Representative experiments are shown (n=4). Cells were transfected as indicated. **D**, Quantitative reverse transcription–polymerase chain reaction analysis for $Ca_v\alpha1.2$ expression in HL1 cells transfected as indicated (n=4). **E**, qRT-PCR analysis for $Ca_v\alpha1.2$ expression in HL1 cells transfected as indicated (n=12). **F, Top**, Consensus $Ca_v\beta2$ DNA-binding motifs in the promoter of the *cacna1c* gene. **Bottom**, Chromatin immunoprecipitation with $Ca_v\beta2$ antibody in HL-1 cells treated as indicated (n=3). **G**, Promoter luciferase assay in HEK293 cells transfected as indicated. All data are shown as mean±SD. Peptide doses were 0.12, 1.3, and 10.2 μmol/L. R7W-scr indicates R7W-scramble. **P*<0.05; ***P*<0.01 (Mann-Whitney test).

analysis confirming the delivery of administered R7W-MP to the heart, the effect of R7W-MP on cardiac function was monitored (Figure VA in the online-only Data Supplement). In vivo echocardiographic analyses revealed no differences between groups (Table I in the online-only Data Supplement), and $Ca_v\alpha1.2$ protein levels were unchanged (Figure VB in the online-only Data Supplement). Furthermore, electrophysiologic properties of isolated adult cardiomyocytes were unaffected (Figure VC–VF in the online-only Data Supplement), and in vivo epicardial multiple lead recording showed no significant changes in cardiac excitability and refractoriness, pointing toward a low index of proarrhythmogenicity (Figure VG in the online-only Data Supplement).

To investigate the potential therapeutic application of R7W-MP, we assessed its effect in a mouse model of streptozotocin-induced diabetes mellitus in which alteration of cardiac contractility and reduced LTCC density are secondary consequences of the disease[10,35–39] (Figure 6A and 6B and Tables II and III in the online-only Data Supplement). Notably, R7W-MP treatment normalized ventricular systolic function and restored $Ca_v\alpha1.2$ protein levels in diabetic mice (Figure 6A and 6B and Table III in the online-only Data Supplement). In addition, functional analyses

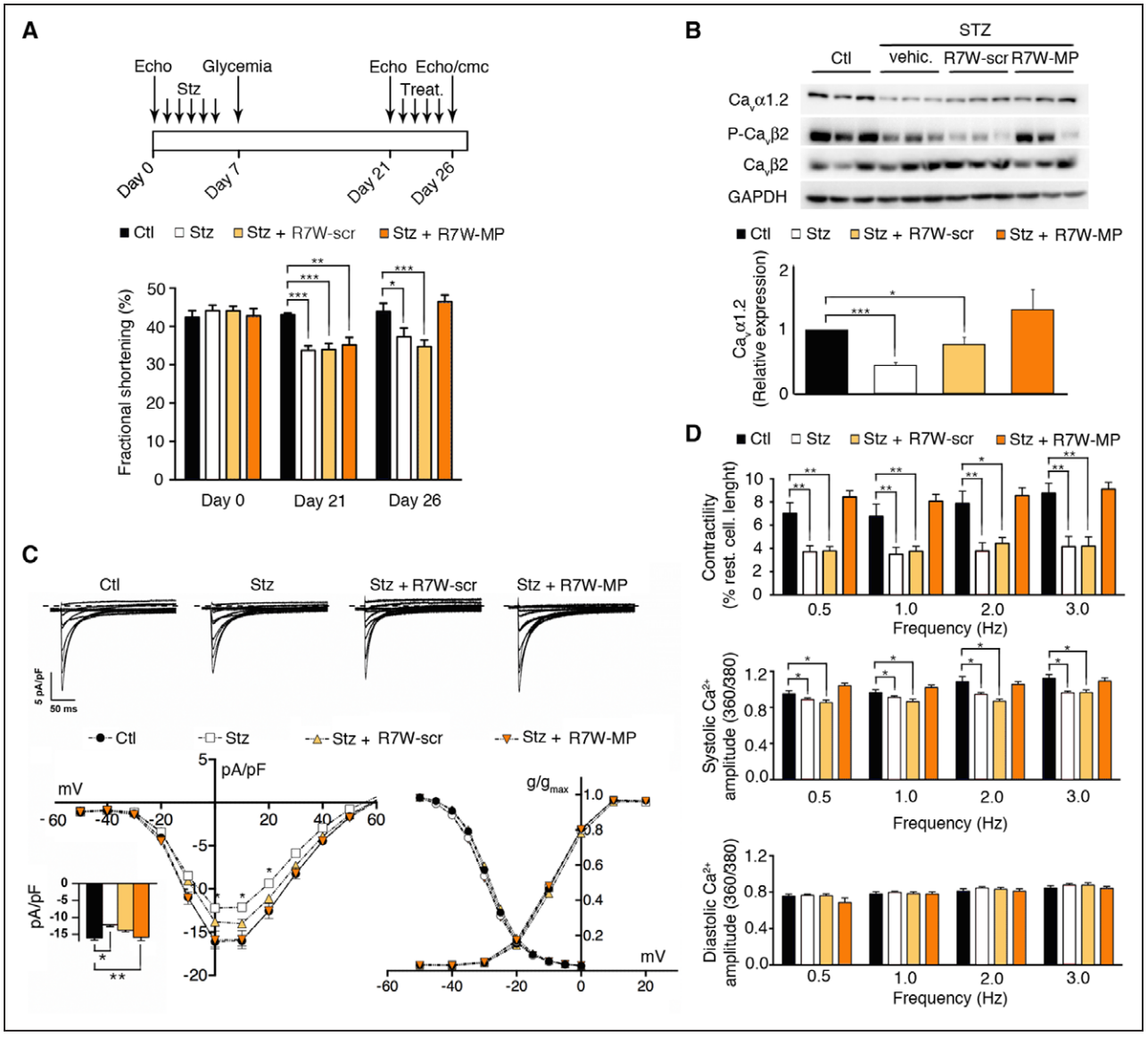


**Figure 6. R7W–mimetic peptide (R7W-MP) restores cardiac function in a mouse model of diabetic cardiomyopathy.** **A**, Design of the study (**top**) and fractional shortening (%; index of heart contraction; **bottom**) as determined by echocardiographic analysis on streptozotocin (Stz)-treated mice injected as indicated (n=10). **B**, Western blot analysis and densitometry for $Ca_v\alpha1.2$, $Ca_v\beta2$, and P-$Ca_v\beta2$ in left ventricular homogenates. **C**, $Ca^{2+}$ current measurements in adult cardiomyocytes isolated from treated mice. Single traces (**top**), I/V relationships (**left bottom**), and steady-state activation/inactivation curves (**right bottom**) are shown (n=15). **D**, Contractility (**top**) and $Ca^{2+}$ transients (**middle**, systolic; **bottom**, diastolic) in adult cardiomyocytes isolated from treated mice at different pacing frequencies (Hz; n=15). Stz and peptides were administered daily by intraperitoneal injection as indicated. All data are shown as mean±SD. R7W-scr indicates R7W-scramble. **P*<0.05; ***P*<0.01; ****P*<0.001 vs control.

of cardiomyocytes from the same mice revealed restoration of cell contractility, systolic $Ca^{2+}$ amplitude, and $I_{Ca,L}$ (Figure 6C and 6D), as well as normalization of $I_{CaL}$ inactivation kinetics (Figure VI in the online-only Data Supplement), in R7W-MP treated mice. These results show the ability of R7W-MP to reduce LTCC turnover and to correct myocardial dysfunction associated with diabetes mellitus, a secondary complication of diabetes mellitus.

On the basis of these outcomes, we explored the potential translatability of our results and retrospectively analyzed left ventricular biopsies from diabetic and nondiabetic cardiomyopathy patients with aortic stenosis undergoing aortic valve replacement. Interestingly, we found a direct linear correlation between the total amount of $Ca_v\alpha1.2$ and the Akt-dependent phosphorylation status of $Ca_v\beta2$ (Figure 7).

## DISCUSSION

The $Ca_v\beta2$ LTCC subunit is known to dictate the appropriate chaperoning of $Ca_v\alpha1.2$ to and density at the

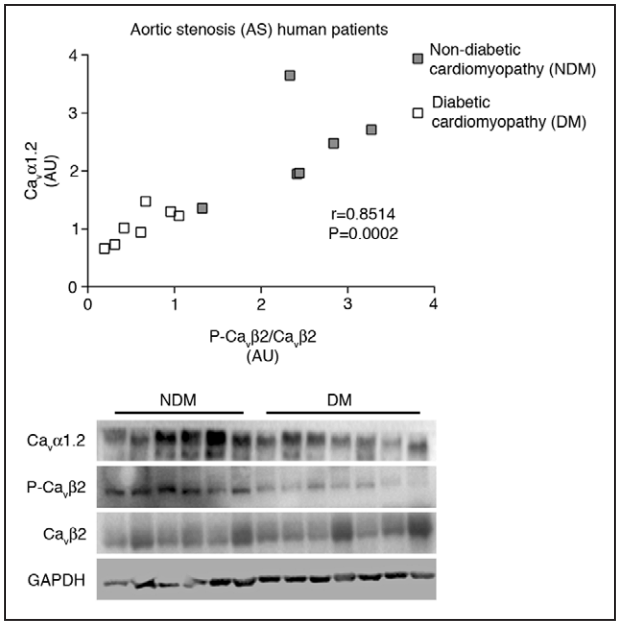


**Figure 7. Phosphorylation status of $Ca_v\beta2$ at the Akt consensus site correlates with $Ca_v\alpha1.2$ levels in the myocardium of patients with diabetic and nondiabetic cardiomyopathy associated with aortic stenosis.**
Densitometry (**top**) and Western blot analysis (**bottom**) on total protein lysates from left ventricular biopsies. A significant correlation was observed (Pearson correlation coefficient). Protein levels were normalized to GAPDH. AU indicates arbitrary units.

cell surface, which is necessary for initiating $Ca^{2+}$ influx and thus proper excitation-contraction coupling in the heart. Under stress conditions, the SH3-dependent scaffolding properties of $Ca_v\beta2$ are altered, thus affecting the assembly, intracellular mobility, and function of the LTCC multiprotein complex. Here, we provide new insights into $Ca^{2+}$ channel physiology and demonstrate that the density of the pore unit is regulated by molecular reorganization of $Ca_v\beta2$, which is initiated by Akt-mediated phosphorylation of its C-terminal tail, allowing it to bind to the central SH3 domain. From this finding, we generated an MP that, by targeting the binding region (TID) within the SH3 domain of $Ca_v\beta2$, increases $Ca_v\alpha1.2$ density at the plasma membrane. Mechanistically, our results point toward a complex regulatory system that involves multiple levels of regulation (Figure 8): reduces $Ca_v\alpha1.2$ retrograde trafficking and protein degradation by preventing dynamin-mediated LTCC endocytosis; promotes $Ca_v\alpha1.2$ anterograde trafficking by blocking Kir/Gem-dependent sequestration of $Ca_v\beta2$, thus facilitating the chaperoning of $Ca_v\alpha1.2$; and promotes $Ca_v\alpha1.2$ transcription by preventing Kir/Gem-mediated shuttling of $Ca_v\beta2$ to the nucleus, where it limits the transcription of $Ca_v\alpha1.2$ through recruitment of the HP1γ epigenetic repressor to the *Cacna1c* promoter. This last mechanism shows that $Ca_v\beta2$ plays a critical role in a previously unknown negative feedback pathway controlling the highly regulated expression of LTCC. Future work should address whether nuclear $Ca_v\beta2$ might be involved in the modulation of a family of genes encoding proteins associated with the regulation of $Ca^{2+}$ handling, sarcomeric assembly, and $Ca^{2+}$ sensitivity of myofilaments, thereby affecting contractility.[34,40–42]

Our results provide the basis for the development of a potential novel therapy for the treatment of car-

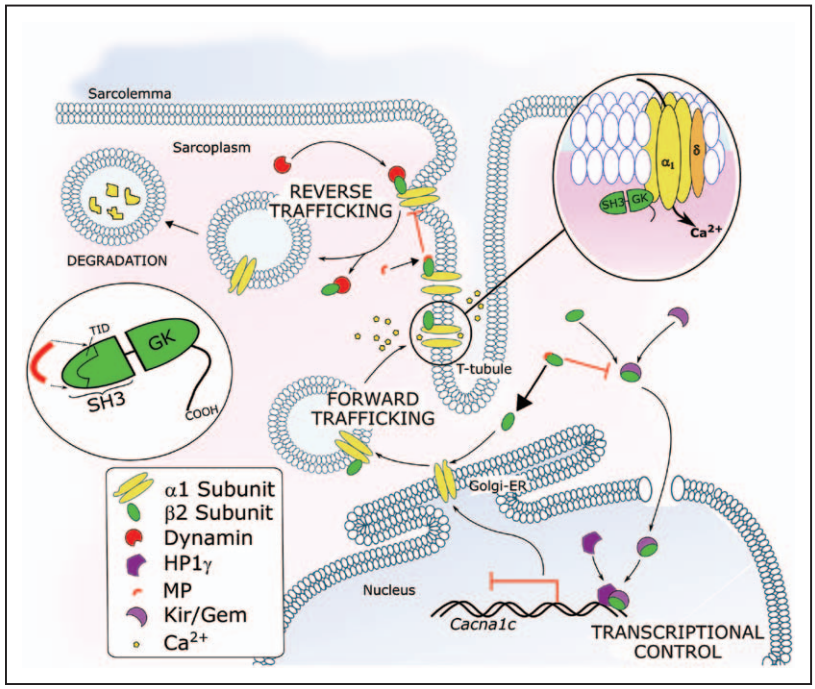


**Figure 8. Working model.**
Mimetic peptide binds to the Src homology 3 (SH3) domain of $Ca_v\beta2$ subunit and facilitates L-type $Ca^{2+}$ channel density at the plasma membrane by promoting forward trafficking, reducing reverse trafficking, and inducing gene expression of $Ca_v\alpha1.2$ subunit. GK indicates guanylate kinase-like; and HP1γ, heterochromatin protein 1γ.

diac disorders associated with reduced LTCC density. The MP generated in this study falls in the class of positive $Ca^{2+}$ modulators, which has received considerable attention in the past decades. However, although remarkably efficient at enhancing $Ca^{2+}$ current and inotropism in systolic heart failure, this class of compounds was also found to favor arrhythmogenesis, thereby limiting their clinical use. For instance, the deleterious effects of the LTCC-activator BAYK8644 was shown to be due at least partly to unwanted modification of gating kinetics of the LTCC pore and $Ca^{2+}$-independent effects on ryanodine receptor gating, increasing resting SR $Ca^{2+}$ release.[43] In contrast, the MP described here acts unconventionally by direct chaperone-mediated modulation of LTCC density and, via its direct action on the life cycle of the channel, restores physiologic levels of LTCC only when its density at the plasma membrane is reduced. Additionally, we found that P-$Ca_v\beta2$ levels, which, as expected, were reduced in diabetic mice, were normalized to control levels after MP treatment. This leads to the intriguing hypothesis that, by binding to $Ca_v\beta2$, MP might facilitate the proximity or availability of the LTCC chaperone for the active Akt at the plasma membrane. If this is the case, in addition to its effect on $Ca_v\alpha1.2$ density at the plasma membrane, MP stimulates the "physiologic" Akt-dependent stabilizing effect on LTCC density and function,[24] thereby initiating a possible forward mechanism. More dedicated and in-depth studies are required to address this possibility. Although an MP-based therapy might be envisioned, as also supported by the striking linear correlation between phosphorylated $Ca_v\beta2$ and $Ca_v\alpha1.2$ density in our preliminary retrospective studies of human patient biopsies, further compound optimization, toxicity studies, and larger-scale prospective analyses are required. For instance, the detrimental effects previously observed with supraphysiologic levels of $Ca_v\beta2$ and $Ca_v\alpha1.2$[44–48] raise the question of whether MP administration may cause similar issues. However, although further and more exhaustive studies are required (ie, short- to long-term pharmacokinetic analysis), it is promising that MP administration did not result in any abnormal increase in $Ca_v\alpha1.2$ density or $I_{Ca,L}$. Additionally, MP did not affect $Ca_v\beta2$ protein levels in either stressed or unstressed conditions. Another issue is the broad tissue distribution of $Ca_v\beta2$, necessitating careful re-evaluation of the nature and type of carrier to use because the current R7W carrier is not specific to the heart and thus may also have potential effects at other locations such as the vasculature or the sympathetic nervous system. In this regard, the recent development of novel drug carriers (ie, cell-specific aptamers[49] or functionalized nanoparticles[50]) might allow specific delivery to the heart and thus minimization of short- or long-term secondary side effects.

## CONCLUSION

This study identifies new regulatory mechanisms controlling the LTCC life cycle and provides proof of concept for a novel therapy for the treatment of cardiac conditions associated with reduced LTCC density.

## ACKNOWLEDGMENTS

We thank A. Rodanò and C. Ronchi for their expertise with animal models and electrophysiologic analysis, respectively; M.V.G. Latronico for graphic preparation; and Dr Emilio Macchi for the helpful discussion about the in vivo electrophysiologic data. HL-1 cells were kindly provided by Dr W. Claycomb; Kir/Gem cDNA by Drs P. Bèguin and S. Seino; and dynamin cDNA by Drs R. Bonecchi and M. Locati.

## SOURCES OF FUNDING

This work was supported by the Cariplo Foundation (2008.2504) and the Italian Ministry of Health (GR-2011-02352546) (DC). Dr Rusconi is supported by the Fondazione Umberto Veronesi Young Investigator Program 2011 to 2012.

## DISCLOSURES

None.

## AFFILIATIONS

From Humanitas Clinical and Research Center, Rozzano, Milan, Italy (F.R., P. Ceriotti, M.M., P. Carullo, N.S., E.D.P., P.K., M.-L.B., G.C., D.C.); Institute of Genetic and Biomedical Research UOS Milan National Research Council, Milan, Italy (F.R., P. Carullo, N.S., E.D.P., M.-L.B., D.C.); Department of Biotechnologies and Biosciences, University of Milan-Bicocca, Milan, Italy (M.R., A.Z.); Departments of Life Sciences (S.R.) and Clinical and Experimental Medicine (M.M.), University of Parma, Parma, Italy; University Hospital of Verona, Division of Cardiac Surgery, Verona, Italy (M.T., G.F.); Department of Sciences, University of Roma Tre, Rome, Italy (S.C., F.P.); University of Montpellier, CNRS UMR 5203, INSERM, Department of Neuroscience, Institute for Functional Genomics, LabEx Ion Channel Science and Therapeutics, Montpellier, France (M.C., J.C.); and National Institute of Nuclear Physics, Rome Tre Section, Rome, Italy (F.P.).

## FOOTNOTES

Received January 19, 2016; accepted June 27, 2016.

The online-only Data Supplement is available with this article at http://circ.ahajournals.org/lookup/suppl/doi:10.1161/CIRCULATIONAHA.116.021347/-/DC1.

*Circulation* is available at http://circ.ahajournals.org.

## REFERENCES

1. Fabiato A, Fabiato F. Use of chlorotetracycline fluorescence to demonstrate Ca2+-induced release of Ca2+ from the sarcoplas-

mic reticulum of skinned cardiac cells. *Nature*. 1979;281:146–148.
2. Bers DM. Cardiac excitation-contraction coupling. *Nature*. 2002;415:198–205. doi: 10.1038/415198a.
3. Best JM, Kamp TJ. Different subcellular populations of L-type Ca2+ channels exhibit unique regulation and functional roles in cardiomyocytes. *J Mol Cell Cardiol*. 2012;52:376–387. doi: 10.1016/j.yjmcc.2011.08.014.
4. Weiss N, Koschak A. *Pathologies of Calcium Channels*. Berlin, Germany; Springer-Verlag; 2014:47–114.
5. Mukherjee R, Hewett KW, Walker JD, Basler CG, Spinale FG. Changes in L-type calcium channel abundance and function during the transition to pacing-induced congestive heart failure. *Cardiovasc Res*. 1998;37:432–444.
6. Takahashi T, Allen PD, Lacro RV, Marks AR, Dennis AR, Schoen FJ, Grossman W, Marsh JD, Izumo S. Expression of dihydropyridine receptor (Ca2+ channel) and calsequestrin genes in the myocardium of patients with end-stage heart failure. *J Clin Invest*. 1992;90:927–935. doi: 10.1172/JCI115969.
7. Christ T, Boknik P, Wöhrl S, Wettwer E, Graf EM, Bosch RF, Knaut M, Schmitz W, Ravens U, Dobrev D. L-type Ca2+ current downregulation in chronic human atrial fibrillation is associated with increased activity of protein phosphatases. *Circulation*. 2004;110:2651–2657. doi: 10.1161/01.CIR.0000145659.80212.6A.
8. Lenaerts I, Bito V, Heinzel FR, Driesen RB, Holemans P, D'hooge J, Heidbüchel H, Sipido KR, Willems R. Ultrastructural and functional remodeling of the coupling between Ca2+ influx and sarcoplasmic reticulum Ca2+ release in right atrial myocytes from experimental persistent atrial fibrillation. *Circ Res*. 2009;105:876–885. doi: 10.1161/CIRCRESAHA.109.206276.
9. He J, Conklin MW, Foell JD, Wolff MR, Haworth RA, Coronado R, Kamp TJ. Reduction in density of transverse tubules and L-type Ca(2+) channels in canine tachycardia-induced heart failure. *Cardiovasc Res*. 2001;49:298–307.
10. Lu Z, Jiang YP, Xu XH, Ballou LM, Cohen IS, Lin RZ. Decreased L-type Ca2+ current in cardiac myocytes of type 1 diabetic Akita mice due to reduced phosphatidylinositol 3-kinase signaling. *Diabetes*. 2007;56:2780–2789. doi: 10.2337/db06-1629.
11. Brugada P, Brugada J, Roy D. Brugada syndrome 1992-2012: 20 years of scientific excitement, and more. *Eur Heart J*. 2013;34:3610–3615. doi: 10.1093/eurheartj/eht113.
12. Goonasekera SA, Hammer K, Auger-Messier M, Bodi I, Chen X, Zhang H, Reiken S, Elrod JW, Correll RN, York AJ, Sargent MA, Hofmann F, Moosmang S, Marks AR, Houser SR, Bers DM, Molkentin JD. Decreased cardiac L-type $Ca^{2+}$ channel activity induces hypertrophy and heart failure in mice. *J Clin Invest*. 2012;122:280–290. doi: 10.1172/JCI58227.
13. Blaich A, Pahlavan S, Tian Q, Oberhofer M, Poomvanicha M, Lenhardt P, Domes K, Wegener JW, Moosmang S, Ruppenthal S, Scholz A, Lipp P, Hofmann F. Mutation of the calmodulin binding motif IQ of the L-type Ca(v)1.2 Ca2+ channel to EQ induces dilated cardiomyopathy and death. *J Biol Chem*. 2012;287:22616–22625. doi: 10.1074/jbc.M112.357921.
14. Mazzanti A, Kanthan A, Monteforte N, Memmi M, Bloise R, Novelli V, Miceli C, O'Rourke S, Borio G, Zienciuk-Krajka A, Curcio A, Surducan AE, Colombo M, Napolitano C, Priori SG. Novel insight into the natural history of short QT syndrome. *J Am Coll Cardiol*. 2014;63:1300–1308. doi: 10.1016/j.jacc.2013.09.078.
15. Catterall WA. Voltage-gated calcium channels. *Cold Spring Harb Perspect Biol*. 2011;3:a003947. doi: 10.1101/cshperspect.a003947.
16. Catterall WA. Structure and regulation of voltage-gated Ca2+ channels. *Annu Rev Cell Dev Biol*. 2000;16:521–555. doi: 10.1146/annurev.cellbio.16.1.521.
17. Singer D, Biel M, Lotan I, Flockerzi V, Hofmann F, Dascal N. The roles of the subunits in the function of the calcium channel. *Science*. 1991;253:1553–1557.
18. Pragnell M, De Waard M, Mori Y, Tanabe T, Snutch TP, Campbell KP. Calcium channel beta-subunit binds to a conserved motif in the I-II cytoplasmic linker of the alpha 1-subunit. *Nature*. 1994;368:67–70. doi: 10.1038/368067a0.
19. Chien AJ, Zhao X, Shirokov RE, Puri TS, Chang CF, Sun D, Rios E, Hosey MM. Roles of a membrane-localized beta subunit in the formation and targeting of functional L-type Ca2+ channels. *J Biol Chem*. 1995;270:30036–30044.
20. Josephson IR, Varadi G. The beta subunit increases Ca2+ currents and gating charge movements of human cardiac L-type Ca2+ channels. *Biophys J*. 1996;70:1285–1293. doi: 10.1016/S0006-3495(96)79685-6.
21. Jones LP, Wei SK, Yue DT. Mechanism of auxiliary subunit modulation of neuronal alpha1E calcium channels. *J Gen Physiol*. 1998;112:125–143.
22. Gonzalez-Gutierrez G, Miranda-Laferte E, Neely A, Hidalgo P. The Src homology 3 domain of the beta-subunit of voltage-gated calcium channels promotes endocytosis via dynamin interaction. *J Biol Chem*. 2007;282:2156–2162. doi: 10.1074/jbc.M609071200.
23. Perez-Reyes E, Castellano A, Kim HS, Bertrand P, Baggstrom E, Lacerda AE, Wei XY, Birnbaumer L. Cloning and expression of a cardiac/brain beta subunit of the L-type calcium channel. *J Biol Chem*. 1992;267:1792–1797.
24. Catalucci D, Zhang DH, DeSantiago J, Aimond F, Barbara G, Chemin J, Bonci D, Picht E, Rusconi F, Dalton ND, Peterson KL, Richard S, Bers DM, Brown JH, Condorelli G. Akt regulates L-type Ca2+ channel activity by modulating Cavalpha1 protein stability. *J Cell Biol*. 2009;184:923–933. doi: 10.1083/jcb.200805063.
25. Mitchell DJ, Kim DT, Steinman L, Fathman CG, Rothbard JB. Polyarginine enters cells more efficiently than other polycationic homopolymers. *J Pept Res*. 2000;56:318–325.
26. Correll RN, Pang C, Niedowicz DM, Finlin BS, Andres DA. The RGK family of GTP-binding proteins: regulators of voltage-dependent calcium channels and cytoskeleton remodeling. *Cell Signal*. 2008;20:292–300. doi: 10.1016/j.cellsig.2007.10.028.
27. Béguin P, Nagashima K, Gonoi T, Shibasaki T, Takahashi K, Kashima Y, Ozaki N, Geering K, Iwanaga T, Seino S. Regulation of Ca2+ channel expression at the cell surface by the small G-protein kir/Gem. *Nature*. 2001;411:701–706. doi: 10.1038/35079621.
28. Yang T, Colecraft HM. Regulation of voltage-dependent calcium channels by RGK proteins. *Biochim Biophys Acta*. 2013;1828:1644–1654. doi: 10.1016/j.bbamem.2012.10.005.
29. Béguin P, Ng YJ, Krause C, Mahalakshmi RN, Ng MY, Hunziker W. RGK small GTP-binding proteins interact with the nucleotide kinase domain of Ca2+-channel beta-subunits via an uncommon effector binding domain. *J Biol Chem*. 2007;282:11509–11520. doi: 10.1074/jbc.M606423200.
30. Hibino H, Pironkova R, Onwumere O, Rousset M, Charnet P, Hudspeth AJ, Lesage F. Direct interaction with a nuclear protein and regulation of gene silencing by a variant of the Ca2+-channel beta 4 subunit. *Proc Natl Acad Sci USA*. 2003;100:307–312.
31. Béguin P, Mahalakshmi RN, Nagashima K, Cher DH, Ikeda H, Yamada Y, Seino Y, Hunziker W. Nuclear sequestration of beta-subunits by Rad and Rem is controlled by 14-3-3 and calmodulin and reveals a novel mechanism for Ca2+ channel regulation. *J Mol Biol*. 2006;355:34–46. doi: 10.1016/j.jmb.2005.10.013.
32. Koonin EV, Zhou S, Lucchesi JC. The chromo superfamily: new members, duplication of the chromo domain and possible role in delivering transcription regulators to chromatin. *Nucleic Acids Res*. 1995;23:4229–4233.
33. Anand P, Brown JD, Lin CY, Qi J, Zhang R, Artero PC, Alaiti MA, Bullard J, Alazem K, Margulies KB, Cappola TP, Lemieux M, Plutzky J, Bradner JE, Haldar SM. BET bromodomains mediate transcriptional pause release in heart failure. *Cell*. 2013;154:569–582. doi: 10.1016/j.cell.2013.07.013.
34. Taylor J, Pereyra A, Zhang T, Messi ML, Wang ZM, Hereñú C, Kuan PF, Delbono O. The Cavβ1a subunit regulates gene expression

and suppresses myogenin in muscle progenitor cells. *J Cell Biol*. 2014;205:829–846. doi: 10.1083/jcb.201403021.
35. Poornima IG, Parikh P, Shannon RP. Diabetic cardiomyopathy: the search for a unifying hypothesis. *Circ Res*. 2006;98:596–605. doi: 10.1161/01.RES.0000207406.94146.c2.
36. Bracken NK, Woodall AJ, Howarth FC, Singh J. Voltage-dependence of contraction in streptozotocin-induced diabetic myocytes. *Mol Cell Biochem*. 2004;261:235–243.
37. Pereira L, Matthes J, Schuster I, Valdivia HH, Herzig S, Richard S, Gómez AM. Mechanisms of [Ca2+]i transient decrease in cardiomyopathy of db/db type 2 diabetic mice. *Diabetes*. 2006;55:608–615.
38. Wang DW, Kiyosue T, Shigematsu S, Arita M. Abnormalities of K+ and Ca2+ currents in ventricular myocytes from rats with chronic diabetes. *Am J Physiol*. 1995;269(pt 2):H1288–H1296.
39. Chattou S, Diacono J, Feuvray D. Decrease in sodium-calcium exchange and calcium currents in diabetic rat ventricular myocytes. *Acta Physiol Scand*. 1999;166:137–144. doi: 10.1046/j.1365-201x.1999.00547.x.
40. Frey N, McKinsey TA, Olson EN. Decoding calcium signals involved in cardiac growth and function. *Nat Med*. 2000;6:1221–1227. doi: 10.1038/81321.
41. Hwang PM, Sykes BD. Targeting the sarcomere to correct muscle function. *Nat Rev Drug Discov*. 2015;14:313–328. doi: 10.1038/nrd4554.
42. Kirk JA, Holewinski RJ, Kooij V, Agnetti G, Tunin RS, Witayavanitkul N, de Tombe PP, Gao WD, Van Eyk J, Kass DA. Cardiac resynchronization sensitizes the sarcomere to calcium by reactivating GSK-3β. *J Clin Invest*. 2014;124:129–138. doi: 10.1172/JCI69253.
43. Katoh H, Schlotthauer K, Bers DM. Transmission of information from cardiac dihydropyridine receptor to ryanodine receptor: evidence from BayK 8644 effects on resting Ca(2+) sparks. *Circ Res*. 2000;87:106–111.
44. Shaw RM, Colecraft HM. L-type calcium channel targeting and local signalling in cardiac myocytes. *Cardiovasc Res*. 2013;98:177–186. doi: 10.1093/cvr/cvt021.
45. Koval OM, Guan X, Wu Y, Joiner ML, Gao Z, Chen B, Grumbach IM, Luczak ED, Colbran RJ, Song LS, Hund TJ, Mohler PJ, Anderson ME. CaV1.2 beta-subunit coordinates CaMKII-triggered cardiomyocyte death and afterdepolarizations. *Proc Natl Acad Sci USA*. 2010;107:4996–5000.
46. Hullin R, Matthes J, von Vietinghoff S, Bodi I, Rubio M, D'Souza K, Friedrich Khan I, Rottländer D, Hoppe UC, Mohacsi P, Schmitteckert E, Gilsbach R, Bünemann M, Hein L, Schwartz A, Herzig S. Increased expression of the auxiliary beta(2)-subunit of ventricular L-type Ca(2)+ channels leads to single-channel activity characteristic of heart failure. *PLoS One*. 2007;2:e292. doi: 10.1371/journal.pone.0000292.
47. Nakayama H, Chen X, Baines CP, Klevitsky R, Zhang X, Zhang H, Jaleel N, Chua BH, Hewett TE, Robbins J, Houser SR, Molkentin JD. Ca2+- and mitochondrial-dependent cardiomyocyte necrosis as a primary mediator of heart failure. *J Clin Invest*. 2007;117:2431–2444. doi: 10.1172/JCI31060.
48. Muth JN, Bodi I, Lewis W, Varadi G, Schwartz A. A Ca(2+)-dependent transgenic model of cardiac hypertrophy: a role for protein kinase Calpha. *Circulation*. 2001;103:140–147.
49. Thiel WH, Esposito CL, Dickey DD, Dassie JP, Long ME, Adam J, Streeter J, Schickling B, Takapoo M, Flenker KS, Klesney-Tait J, Franciscis Vd, Miller FJ Jr, Giangrande PH. Smooth muscle cell-targeted RNA aptamer inhibits neointimal formation. *Mol Ther*. 2016;24:779–787. doi: 10.1038/mt.2015.235.
50. Di Mauro V, Iafisco M, Salvarani N, Vacchiano M, Carullo P, Ramírez-Rodríguez GB, Patrício T, Tampieri A, Miragoli M, Catalucci D. Bioinspired negatively charged calcium phosphate nanocarriers for cardiac delivery of MicroRNAs. *Nanomedicine (Lond)*. 2016;11:891–906. doi: 10.2217/nnm.16.26.